DOI: 10.1002/ejic.200500978

A Series of One- to Three-Dimensional Copper Coordination Polymers Based on N-Heterocyclic Ligands

Xiang He,[a] Can-Zhong Lu*[a] Chuan-De Wu,[a] and Li-Juan Chen[a]

Keywords: Coordination polymers / Copper / Luminescence / Nitrogen heterocycles / Organic–inorganic hybrid composites

A family of copper coordination polymers containing different N-heterocyclic ligands, namely $[Cu(CN)(dmpyz)]_n$ (**1**), $[Cu_2(CN)_2(imz)]_n$ (**2**), $[Cu_3(CN)(trz)_2]_n$ (**3**), $[Cu_6(CN)_6(dmtrz)_3]_n$ (**4**), $[Cu_2(CN)(5\text{-metta})]_n$ (**5**), $[Cu_2(CN)(5\text{-phtta})]_n$ (**6**), and $\{[Cu_6(CN)_6(dmtrz)]_2[Cu_2(CN)_2(dmtrz)_2]\}_n$ (**7**) has been prepared and structurally characterized by X-ray crystallography. The crystal structures of **1** and **2** are 1D chain frameworks. Compound **3** is a twofold interpenetrating 2D supramolecular framework in which the cyanide groups act as bridging ligands to link the copper centers into an unusual bilayer motif with large channels. Compounds **4**–**6** all possess 3D networks. Compound **4** is constructed by two parts: 2D rectangular-grid layers and $\{Cu_2(CN)_2(dmtrz)_2\}$ building blocks. Compound **5** is built up by X-shaped chains that connect each other in an ABAB arrangement to generate the 3D network. The structure of **6** is a 3D network including one-dimensional square-grid channels, with a shortest Cu2···Cu2A (A: $-x + 1, -y + 1, -z$) distance of about 2.347(1) Å. Compound **7** features a peculiar 3D + 1D network in which 1D guest metal-organic polymer chains are filled in an unusual 3D architecture constructed by double helical host tubes. Compounds **1**–**7** show a systematic variation in dimensionality from 1D to 3D to 3D + 1D. The luminescence properties of these compounds have been also studied.

Introduction

Considerable attention has been paid to the study of metal coordination polymers not only because these polymers may possess intriguing architectures but also because of their potential applications in the fields of catalysis, molecular-based magnets, electrical conductivity, and zeolite-like materials.[1–3] Among these metal coordination polymers, copper cyanide systems have received special interest due to their fascinating structural frameworks, physical and chemical properties, and potential applications in many fields.[4–7] When studied from a coordination chemistry viewpoint, the structural variety of copper cyanide coordination polymers might be the result of two main factors. Firstly, the cyanide group is a versatile ligand that can act as a monodentate ligand as well as a μ_2-, μ_3-, or μ_4-bridging ligand to generate interesting compounds that may exhibit intriguing topological architectures.[8,9] Secondly, the copper atom has versatile coordination properties and normally adopts three-, four-, five-, or six-coordination to form diverse geometries; the ligand geometry also plays an important role in controlling the structural dimensionalities and stereochemistry of the copper center.[10] On the other hand, from a synthetic chemistry viewpoint, cyanide-containing systems may be prepared either by assembling cyanometalates and metal complexes or by multicomponent self-assembly of cyanide, metal ions, and multidentate ligands. Although the majority of synthetic processes in these systems still follow the conventional solution route, attention has recently turned to solvothermal techniques.[11] To understand the construction of supramolecular architectures further, it is important to continue the investigations on the effect of organic ligands when fabricating multidimensional polymers. We are currently interested in using CuCN, $K_3Fe(CN)_6$, and a series of five-membered N-heterocyclic ring ligands (Scheme 1) as precursors to obtain some homometallic cyanide-bridged coordination polymeric compounds under hydrothermal conditions. In this article we report seven copper polymeric compounds, namely $[Cu(CN)(dmpyz)]_n$ (**1**), $[Cu_2(CN)_2(imz)]_n$ (**2**), $[Cu_3(CN)(trz)_2]_n$ (**3**), $[Cu_6(CN)_6(dmtrz)_3]_n$ (**4**) $[Cu_2(CN)(5\text{-metta})]_n$ (**5**), $[Cu_2(CN)(5\text{-phtta})]_n$ (**6**), and $\{[Cu_6(CN)_6(dmtrz)]_2[Cu_2(CN)_2(dmtrz)_2]\}_n$ (**7**), which exhibit variation dimensionalities.

[a] State Key Laboratory of Structural Chemistry, Fujian Institute of Research on the Structure of Matter, the Chinese Academy of Sciences,
Fuzhou, Fujian 350002, China
Fax: +86-591-8371-4946
E-mail: czlu@ms.fjirsm.ac.cn
Supporting information for this article is available on the WWW under http://www.eurjic.org or from the author.

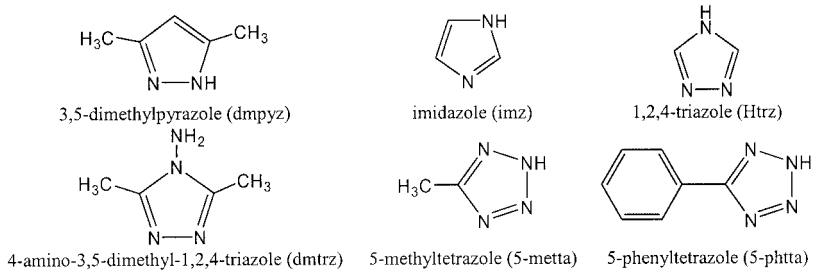

Scheme 1.

Results and Discussion

Synthetic Considerations

In order to study the overall factors affecting the structural frameworks of the cyanide-bridged systems, we varied the reaction conditions (including reagent, temperature, and metal/ligand ratio). Firstly, we used $K_3Fe(CN)_6$ as a precursor instead of KCN to provide CN^-, based on the following consideration: (1) free cyanide might be released from the dissociation of ferricyanide anions under hydrothermal conditions; (2) the slow release of CN^- might play an important role in the formation of various compounds; (3) cyanide-bridged iron(II)–copper(I) dimetallic compounds might be obtained under appropriate conditions.[12] Secondly, different kinds of N-heterocyclic ligands have an important impact on the final structures of the compounds obtained. Thirdly, the role of temperature in determining the structures of the products can be observed. Under hydrothermal conditions, we used $K_3Fe(CN)_6$ as a precursor to successfully obtain these new cyanide-bridged copper coordination polymers. Compound **7** is obtained at 180 °C, while at a lower temperature of 140 °C, violet, plate-like crystalline $K[Cu(CN)_3]_n{\cdot}H_2O$[13,14] is obtained instead of compound **7**. Interestingly, varying the composition of the reaction mixture gives **4** instead of **7**. During the synthesis of compound **3**, when $CuCl_2$ is used instead of CuCN under otherwise identical reaction conditions compound **3** is again obtained. The design and synthesis of novel coordination architectures controlled by varying the reaction conditions (including temperature,[15] metal/ligand ratio,[16] and counteranions[17]) are of great interest in coordination chemistry.

Crystal Structures

[Cu(CN)(dmpyz)]$_n$ (1)

As shown in Figure 1, the structure exhibits a backbone constructed by a zigzag {Cu(CN)} chain. Each Cu^I ion is in a trigonal-planar geometry, defined by one nitrogen atom from the 3,5-dimethylpyrazole ligand [Cu(1)–N(1) = 1.988(7) Å] and two cyanide groups [Cu(1)–X(6) = 1.870(11), Cu(1)–X(7) = 1.986(8) Å; X(6)–Cu(1)–X(7A) = 125.0(4)°], which bridge neighboring copper atoms to form the parent chain. The distance between the aromatic rings of the 3,5-dimethylpyrazole ligands from adjacent chains is 3.221 Å, which indicates the presence of a π–π stacking interaction.

[Cu$_2$(CN)$_2$(imz)]$_n$ (2)

The structure of **2** is similar to that of **1**, as shown in Figure 2. This compound contains two coordination modes for the Cu^I ions: one is coordinated by three cyanide groups [Cu(1)–X(1) = 1.916(5), Cu(1)–X(2) = 1.920(4) Å; X(1)–Cu(1)–X(2) = 119.94(14)°], and the other is nonlinearly coordinated by one cyanide group and one imidazole ligand [Cu(2)–X(3) = 1.843(6), Cu(2)–N(4) = 1.877(5) Å; N(4)–Cu(2)–X(3) = 170.1(3)°]. The structure also exhibits a backbone constructed from a zigzag {Cu(CN)} chain, with [Cu(CN)(imz)] groups projecting from the chain as side-arms.

[Cu$_3$(CN)(trz)$_2$]$_n$ (3)

The structure of **3** is an interesting twofold interpenetrated 2D supramolecular framework. As shown in Figure 3, the structure of **3** possesses six unique metal sites. Three metal centers [Cu(2), Cu(3), and Cu(5)] are all in distorted trigonal geometries. However, the detailed coordination environment of these copper atoms is different as Cu(2) and Cu(5) are coordinated by two triazole ligands and one μ_2-bridging cyanide group while Cu(3) is coordinated by two triazole ligands and one μ_3-1,2κC:3κN cyanide group, with Cu–X bond lengths ranging from 1.881(10) to 1.889(9) Å, and a Cu(3)–N_{CN} bond length of 1.886(10) Å. Cu(1) is in a tetrahedral geometry and is coordinated by two triazole ligands and two μ_3-1,2κC:3κN cyanide groups [Cu(1)–C(3) = 2.221(11) Å], the Cu(1)–C(3) bond being much longer than that to the μ_2-bridging cyanide group. The remaining sites [Cu(4) and Cu(6)] are in linear geometries and are coordinated by two triazole ligands with N–Cu–N bond angles of 178.1(4)° and 176.7(4)°, respectively.

The $\{Cu_2N_4\}$ ring formed by atoms Cu(3) and Cu(5) [or Cu(1) and Cu(2)] and the 1- and 2-nitrogen donors of the trz ligands is nonplanar, and the dihedral angle between the Cu(3)Cu(5)N(6)N(7) and Cu(3)Cu(5)N(6B)N(7B) moieties is 20.85(12)°. Cu(3) and Cu(5) are bridged by two trz ligands with a Cu···Cu separation of 3.5316(16) Å, and these ligands bond through their N^4 sites to Cu(4) to form a two-coordinate linear geometry, which means that the deprotonated triazole binds in a μ_3-bridging mode to link the copper

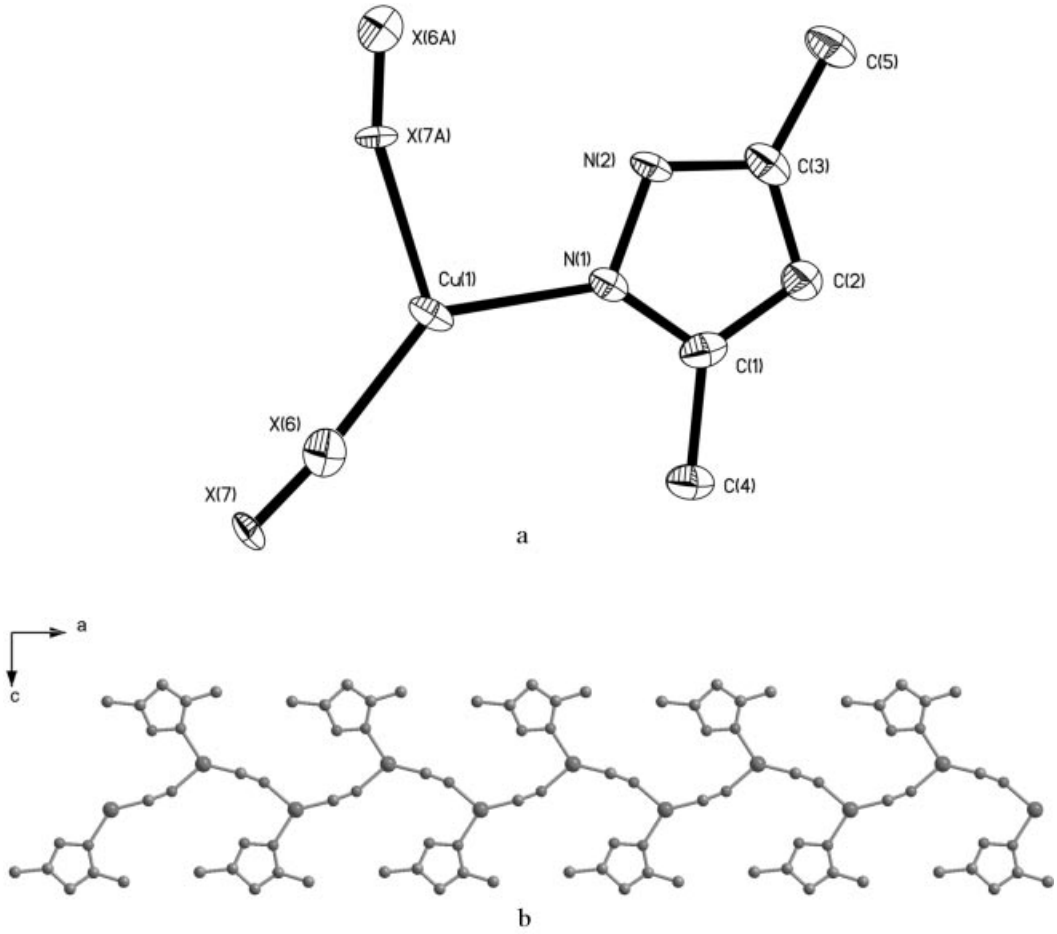

Figure 1. (a) ORTEP representation of the polymeric structure of **1**, showing the coordination environments of the Cu centers (30% probability thermal ellipsoids; hydrogen atoms have been omitted for clarity). Atoms from the disordered CN bridging groups are labeled as X. (b) Schematic view of the chain of **1** viewed along the *b* axis.

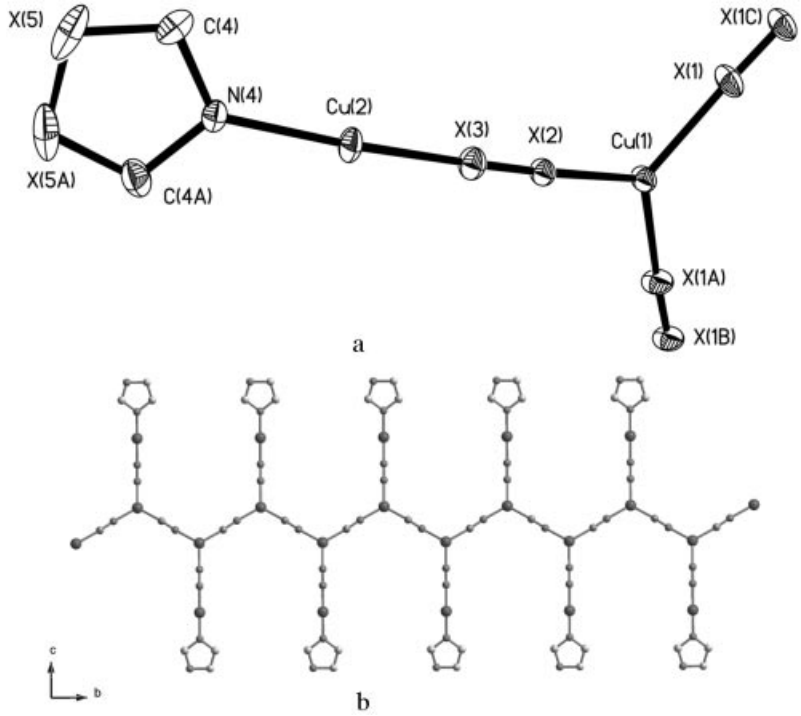

Figure 2. (a) ORTEP representation of the polymeric structure of **2**, showing the coordination environments of the Cu centers (30% probability thermal ellipsoids; hydrogen atoms have been omitted for clarity). Atoms from the disordered CN bridging groups are labeled as X. (b) Schematic view of the chain of **2** viewed along the *a* axis.

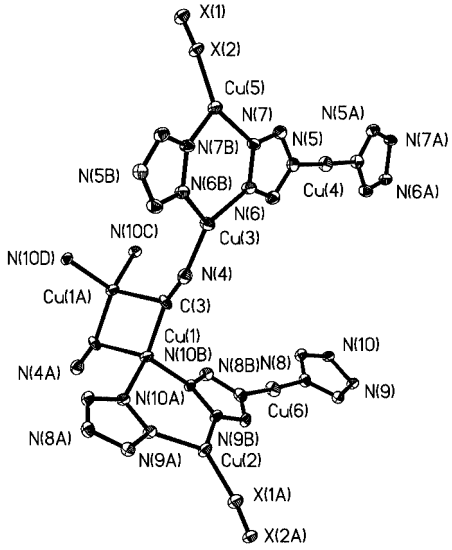

Figure 3. ORTEP representation of the polymeric structure of **3**, showing the coordination environments of the Cu centers (30% probability thermal ellipsoids; hydrogen atoms have been omitted for clarity). Atoms from the disordered CN bridging groups are labeled as X.

ions into linear chains along the *b* axis, with Cu(4), Cu(3), and Cu(5) in one chain and Cu(6), Cu(2), and Cu(1) in the other. In addition, the cyanide groups not only act as μ_2-bridges to link these chains into a wave-like layer structure but also as μ_3-bridges to link Cu(1) and Cu(6) from two different layers together to form an unusual bilayer motif (Figure 4a), which exhibits large channels with dimensions of approximately 11.69×13 Å^2 along the *b* axis. These bilayers pass through each other to generate the interpenetrating 2D network (Figure 4b). In addition, there are π–π stacking interactions between adjacent aromatic rings of triazole ligands with a separation of about 3.299 Å.

Although several types of double-layered architectures have been reported by the assembly of T-shaped or rectangular building blocks,[18–20] this ring-shaped network, to the best of our knowledge, is unprecedented. A view along the *b* axis shows that the actual crystal structure of **3** is a twofold interpenetrating 2D supramolecular framework (Figure S1). This is consistent with the fact that crystal structures with such large cavities are stabilized either by inclusion of suitable guests or by interpenetrating lattices.[21]

[Cu$_6$(CN)$_6$(dmtrz)$_3$]$_n$ (4)

The 3D network of compound **4** is made up of two parts: one is a 2D rectangular grid layer and the other is a $\{Cu_2(CN)_2(dmtrz)_2\}$ building block. As shown in Figure 5, the crystal structure has six crystallographically independent Cu atoms bridged by cyanide groups and dmtrz ligands. The copper atoms adopt two kinds of coordination modes, namely three- and four-coordination. Cu(2), Cu(3), Cu(6), and Cu(1) are in distorted trigonal geometries, of

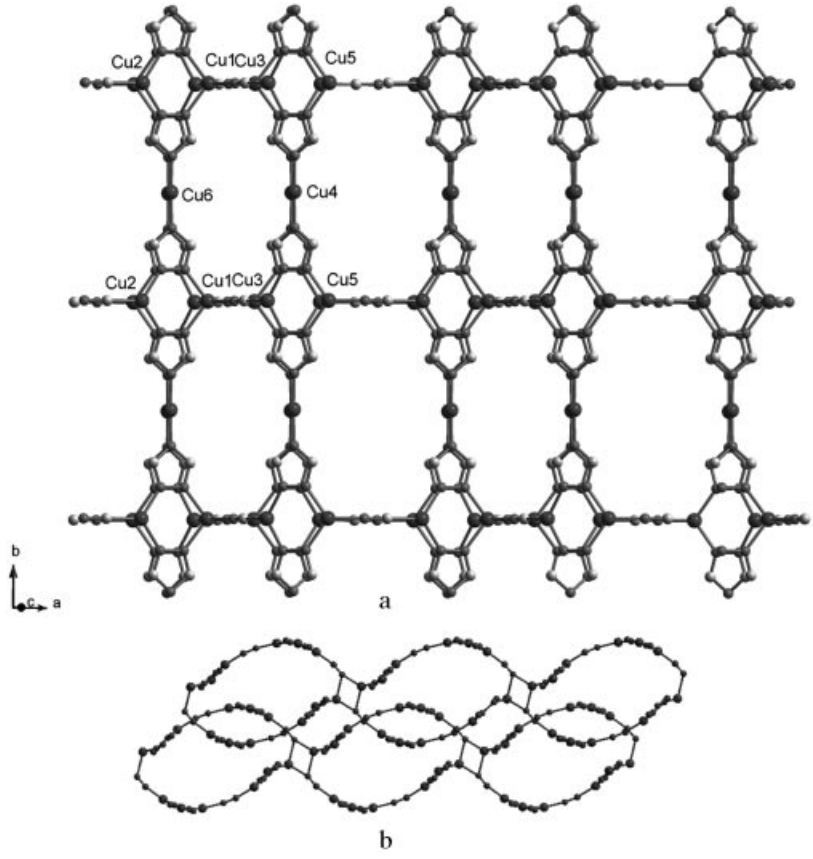

Figure 4. (a) Layer structure of compound **3**. (b) Interpenetrating 2D network constructed by the bilayers, with a large channel of approximately 11.69×13 Å^2, viewed along the *b* axis.

which the former three are three-coordinated by two dmtrz ligands [Cu–N_{dmtrz} = 1.967(3)–2.014(3) Å] and one μ_2-bridging cyanide group, with Cu–X bond lengths ranging from 1.888(4) to 1.895(4) Å, while Cu1 is coordinated by three cyanide groups, two of the being in μ_2-bridging modes [Cu–X = 1.899(4)–1.992(4) Å] and the other in a μ_3-bridging mode [Cu(1)–N(14) = 1.896(3) Å]. Cu(4) and Cu(5) are both in tetrahedral geometries and are coordinated to four cyanide groups. However, the coordination environments of these two copper atoms are different as Cu(4) is coordinated by two μ_3-bridging [Cu(4)–C(20) = 2.055(4), Cu(4)–C(20A) = 2.142(4) Å] and two μ_2-bridging cyanide groups [Cu(4)–X = 1.967(3)–2.007(3) Å], while Cu(5) is coordinated by three μ_3-bridging and one μ_2-bridging cyanide groups.

In the $\{Cu_2(CN)_2(dmtrz)_2\}$ building block (Figure 6a), the $\{Cu_2N_4\}$ ring formed by the *endo* Cu atoms and the 1- and 2-nitrogen donors of the dmtrz ligands is almost planar, with a dihedral angle between the Cu(2)Cu(3)N(5)N(6) and Cu(2)Cu(3)N(1)N(2) planes of 5.23(7)°. The adjacent Cu(2)Cu(3)N(5)N(6)N(1)N(2) and Cu(6)Cu(6A)N(9)N(10)N(9A)N(10A) ring planes in this building block are nearly parallel, with a dihedral angle of 3.519°.

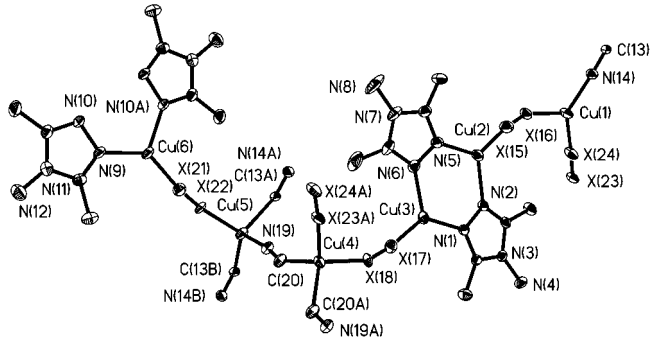

Figure 5. ORTEP representation of the polymeric structure of **4**, showing the coordination environments of the Cu centers (30% probability thermal ellipsoids; hydrogen atoms have been omitted for clarity). Atoms from the disordered CN bridging groups are labeled as X.

The structure consists of 2D rectangular grid layers (Figure 6b), parallel to the *ab* plane, constructed by six-mem-

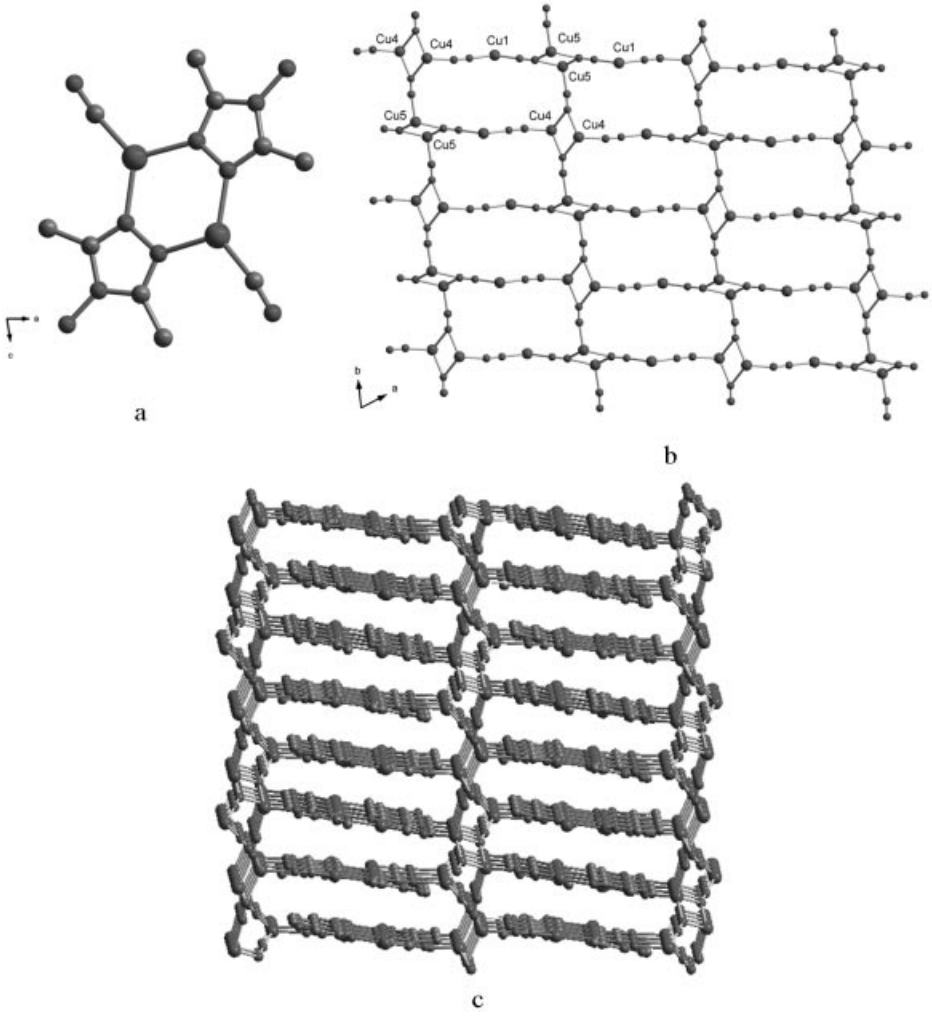

Figure 6. (a) $\{Cu_2(CN)_2(dmtrz)_2\}$ building block. (b) 2D rectangular grid layers. (c) 3D framework of compound **4** constructed by parallel 2D rectangular grid layers linked by the $\{Cu_2(CN)_2(dmtrz)_2\}$ building block.

bered nonplanar centrosymmetric rings of metal atoms in which the metal centers are bridged by cyanide groups. These rings all adopt a chair conformation for the Cu4–Cu1–Cu5–Cu4′–Cu1′–Cu5′ unit, with a ring size of 8.9×8.0 Å^2. The strong Cu···Cu interaction, with a separation of 2.442(8) Å, is double-bridged by two cyanide groups. Although the shortest known Cu^I···Cu^I separation is 2.412(1) Å,[22] the Cu···Cu distance in the present compound is notably shorter than those found in other Cu^I compounds[23] that show strong Cu···Cu interactions.

The parallel 2D rectangular grid layers are linked by $\{Cu_2(CN)_2(dmtrz)_2\}$ building blocks to form a 3D framework (Figure 6c and Figure S2); π–π stacking interactions are present between adjacent $\{CuN_4\}$ planes in compound **4**, with a plane–plane separation of about 3.327 Å and a centroid–centroid distance of 3.407 Å.

[Cu$_2$(CN)(5-metta)]$_n$ (5)

The structure of **5** is a 3D supramolecular framework composed of X-shaped one-dimensional chains. As shown in Figure 7, the structure consists of two crystallographically independent Cu atoms that adopt two kinds of coordination modes, namely three- and four-coordination. Cu(1) trigonally coordinates to two N atoms from different 5-metta ligands and one N atom from a μ_3-bridging cyanide group, while Cu(2) is tetrahedrally coordinated by two N atoms from two 5-metta ligands and two C atoms from different μ_3-bridging cyanide groups. The X-shaped one-dimensional chains are formed by copper atoms bridged by 5-metta ligands in a μ_4-tetrazolyl mode with a Cu2···Cu2B

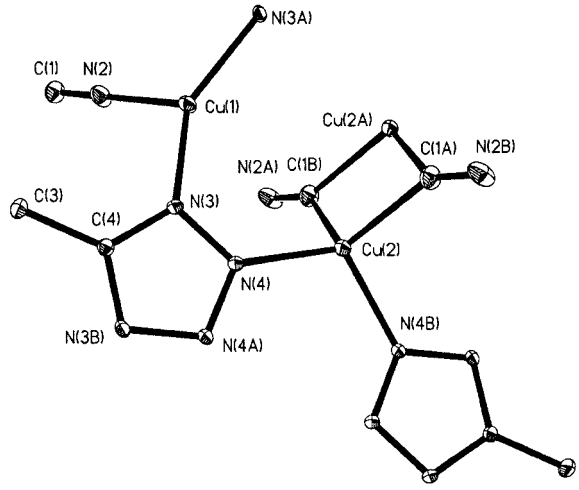

Figure 7. ORTEP representation of the polymeric structure of **5**, showing the coordination environments of the Cu centers (30% probability thermal ellipsoids; hydrogen atoms have been omitted for clarity). Atoms from the disordered CN bridging groups are labeled as X.

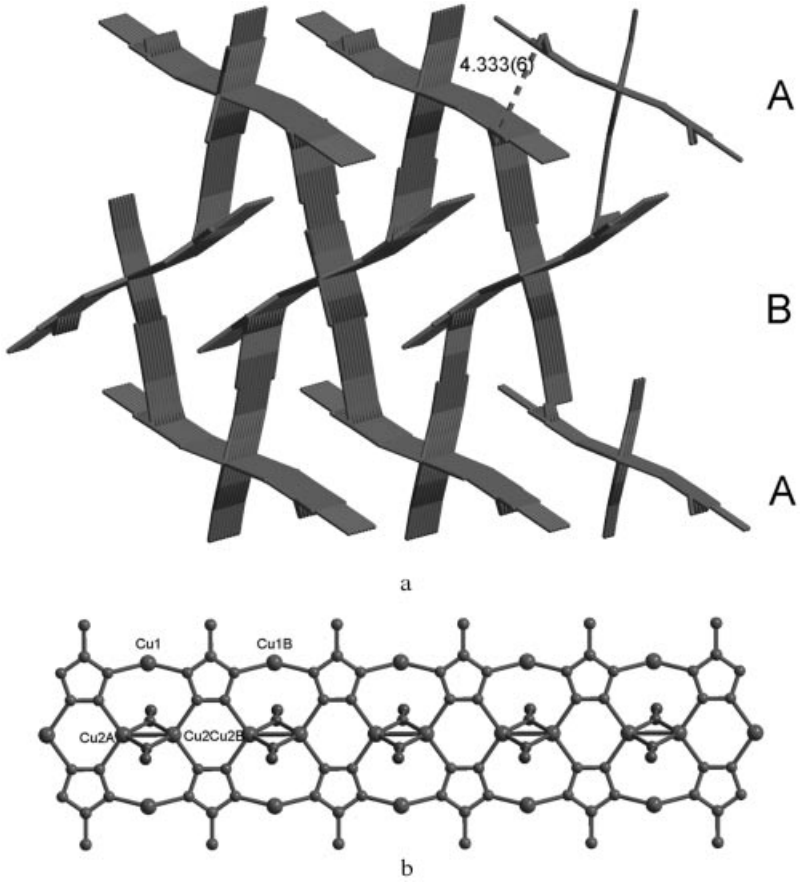

Figure 8. (a) 3D structure constructed by the X-shaped one-dimensional chains. (b) One-dimensional chain bridged by 5-metta ligands and cyanide groups [Cu2···Cu2A (A: $x + 1$, $y + 1$, z) = 2.347(1) Å].

(B: x, y, $-z + 1$) distance of 3.586(1) Å and a Cu1···Cu1B (B: x, y, $-z + 1$) distance of 5.933(7) Å and two cyanide groups doubly bridging Cu2···Cu2A (A: $-x + 1$, $-y + 1$, $-z$) with a distance of 2.347(1) Å. Rare examples with such short values have been found for other Cu^{I} compounds.[24] The adjacent chains are parallel to each other in the same layer, with a Cu···Cu distance of 4.333(6) Å, while they are linked by a cyanide group between adjacent layers (Figure 8). These X-shaped chains connect to each other in an ABAB arrangement to generate an interesting 3D network (Figure S3); π–π stacking interactions between adjacent aromatic rings of tetrazole also exist in compound **5**, with a plane–plane separation of about 3.370 Å.

[Cu$_2$(CN)(5-phtta)]$_n$ (6)

The structure of **6** is a 3D network (Figure 9). There is one crystallographically independent Cu^{I} center, which adopts three-coordination in a distorted trigonal geometry, coordinated by two μ_4-5-phtta ligands and one μ_2-cyanide group [N_{phtta}–Cu(1) = 1.966(2)–2.0867(18), X–Cu(1) = 1.876(2) Å; N(X)–Cu(1)–N(X) = 102.88(7)–140.47(9)°]. The 5-phtta ligands bind in a μ_4-tetrazolyl mode to bridge four copper atoms to form a one-dimensional chain with a Cu···Cu separation of 3.512(2) and 3.794(2) Å along the c axis (Figure 10a). Each chain is bridged by a cyanide group to form a square-grid structure that exhibits large channels with approximate dimensions of 8.472 × 9.259 Å^2, although the effective pore size is partly reduced by the phenyl groups of the 5-phtta ligands Furthermore, these one-dimensional chains are linked to each other by cyanide groups to form the 3D framework (Figure 10b and Figure S4).

{[Cu$_6$(CN)$_6$(dmtrz)]$_2$[Cu$_2$(CN)$_2$(dmtrz)$_2$]}$_n$ (7)

The crystal structure of **7** is comprised of two distinct and crystallographically independent polymeric motifs packed together to form a 3D architecture, which comprises interesting double helical host tubes filled by 1D metal-organic polymeric chains as guests, i.e. {[$Cu_6(CN)_6$(dmtrz)]$_n$}$_2$ (**A**) and [$Cu_2(CN)_2$(dmtrz)$_2$]$_n$ (**B**).

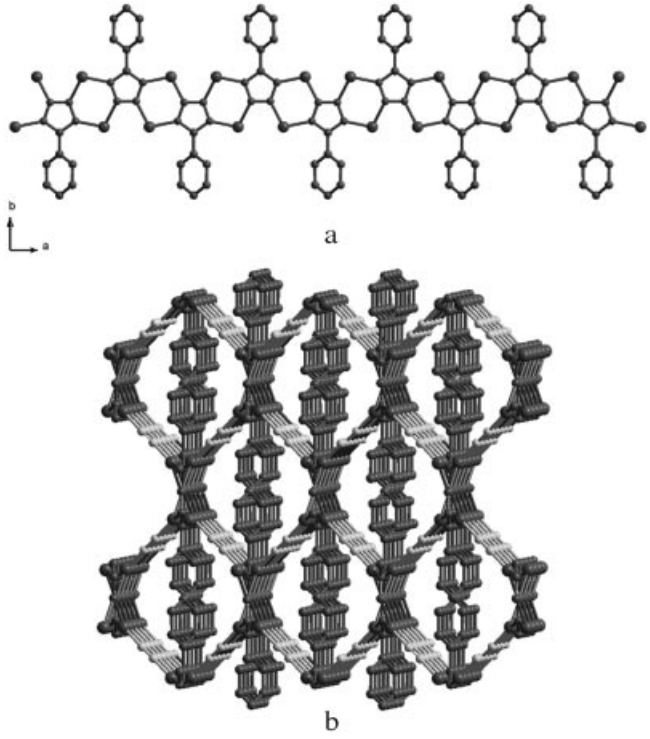

Figure 10. (a) One-dimensional chain constructed by 5-phtta ligands. (b) 3D structure of compound **6**.

The crystal structure has six crystallographically independent Cu atoms bridged by cyanide groups and a dmtrz ligand in polymer **A** (Figure 11). The copper atoms adopt two kinds of coordination modes, namely two- and three-coordination. Cu4, Cu5, and Cu6 are in linear geometries, coordinated by two μ_2-bridging cyanide groups [Cu–X = 1.839(4)–1.866(4) Å; X–Cu–X = 166.3(2)–170.4(2)°], while Cu7 and Cu8 are in distorted trigonal geometries and are coordinated by three μ_2-bridging cyanide groups [Cu–X = 1.895(4)–1.993(4) Å; X–Cu–X = 111.21(18)–133.42(18)°], while Cu3 is also in a distorted trigonal geometry and is

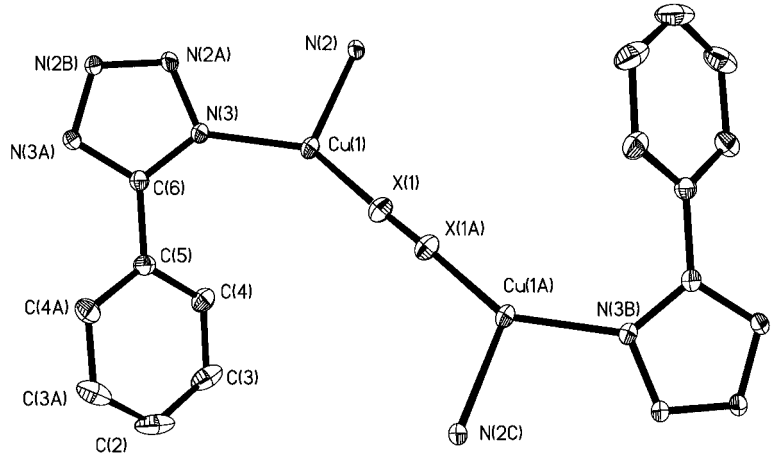

Figure 9. ORTEP representation of the polymeric structure of **6**, showing the coordination environments of the Cu centers (30% probability thermal ellipsoids; hydrogen atoms have been omitted for clarity). Atoms from the disordered CN bridging groups are labeled as X.

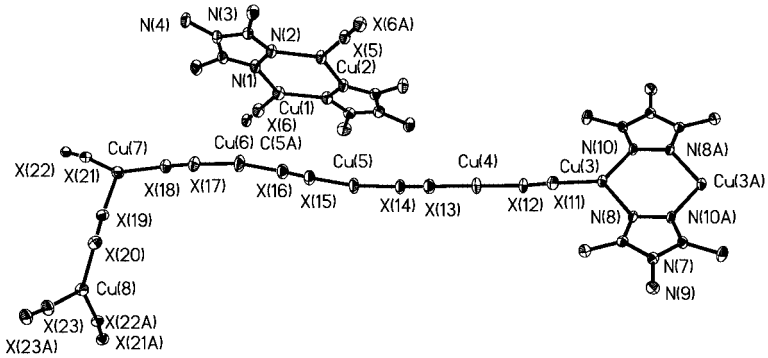

Figure 11. ORTEP representation of the polymeric structure of **7**, showing the coordination environments of the Cu centers (30% probability thermal ellipsoids; hydrogen atoms have been omitted for clarity). Atoms from the disordered CN bridging groups are labeled as X.

coordinated by two dmtrz ligands [Cu3–N_{dmtrz} = 1.967(3)–2.014(3) Å] and one μ_2-bridging cyanide group [Cu3–X11 = 1.886(4) Å] The host polymer **A** consists of two kinds of helical chains, namely mode I and mode II (Figure 12a). Six copper atoms bridged by six cyanide ions form a honeycomb-shaped helical chain (mode I) when viewed along the *b* axis. The unclosed Cu–CN linkage in this structure gives rise to two types of helices with opposite chiralities (Figure S5). The left- and right-handed helices are coupled with each other to form helical tubes of approximately 4.99×5.00 Å^2 with opposite chirality (calculated from opposite metal ion centers of the hexagon; Figure 12b). The helical chain along the 2_1 screw axis has a long pitch of 12.898(1) Å (Figure 13a). The helical chain of mode II is composed of 22 copper atoms bridged by 20 cyanide ions and four dmtrz ligands to form a distorted hexagon. To the best of our knowledge, this is the first compound constructed from such a long chain of cyanide-bridged copper atoms. The left- and right-handed helical chains of mode II form helical channels of 42.26×4.99 Å^2 with opposite chirality (calculated from the opposite metal ions of the hexagon). The long pitch of the helical chain along the 2_1 screw axis is 59.985(6) Å (Figure 13b). Two chemically independent polymers **A** interweave to form a 3D architecture with double-stranded helical channels along two spiral directions (Figure S6).

There are two crystallographically independent Cu atoms bridged by cyanide groups and dmtrz ligand in polymer **B**

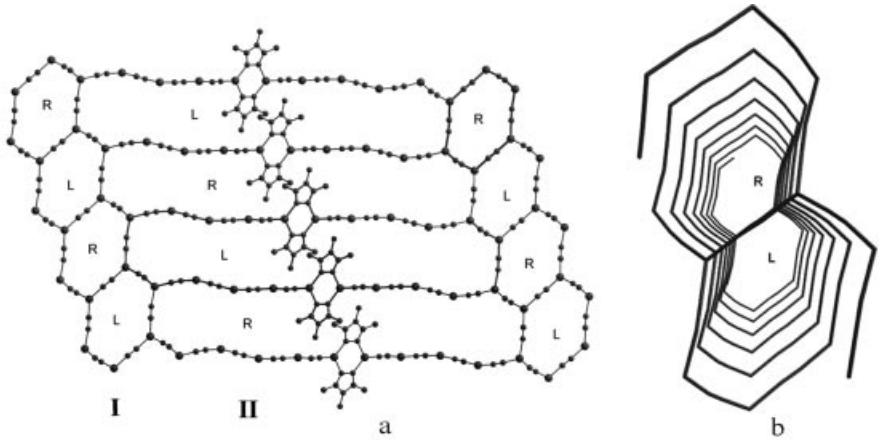

Figure 12. (a) Two kinds of helical chains (modes I and II) in polymer **A**. (b) Right- and the left-handed helical tubes of mode I.

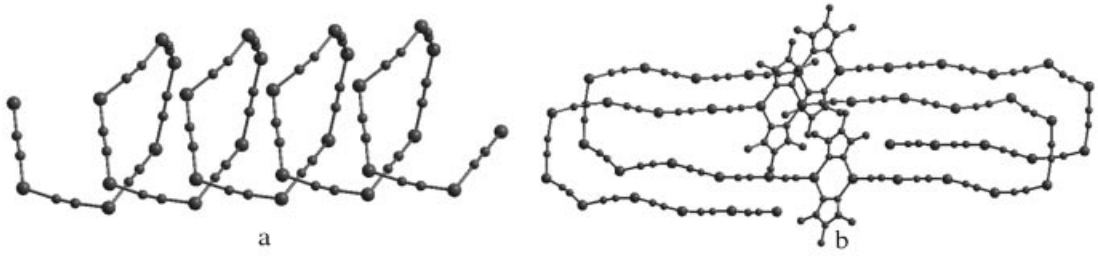

Figure 13. (a) Structure of a helical chain of mode I with a pitch of 12.898(1) Å running along the screw axis. (b) Structure of a helical chain of mode II with a pitch of 59.985(6) Å running along the screw axis.

(Figure 14). Cu1 and Cu2 are in distorted trigonal geometries and are coordinated by two dmtrz ligands [Cu–N_{dmtrz} = 1.967(3)–2.014(3) Å] and one μ_2-bridging cyanide group [Cu–X = 1.885(5)–1.897(6) Å], with Cu···Cu separations of 3.652(1) Å. These building blocks are linked further by cyanide ions to form cable-like linear chains. The polymers **B** are present in the helical channels with opposite chirality constructed by helical chains of mode II. The guest polymers play an important role in the formation of double-stranded helical channels through specific host–guest interactions (Figure 15).

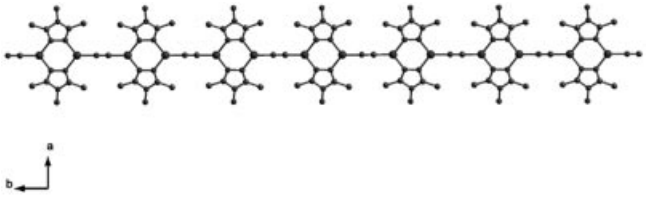

Figure 14. One-dimensional chain of polymer **B**.

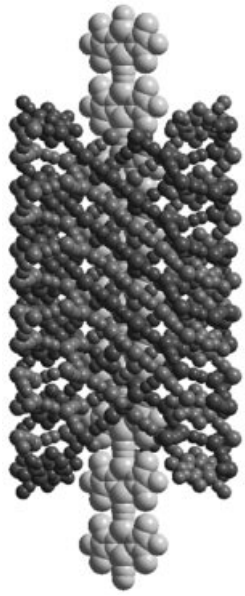

Figure 15. One-dimensional chain of polymer **B** filled in the mode II helical channel of polymer **A**.

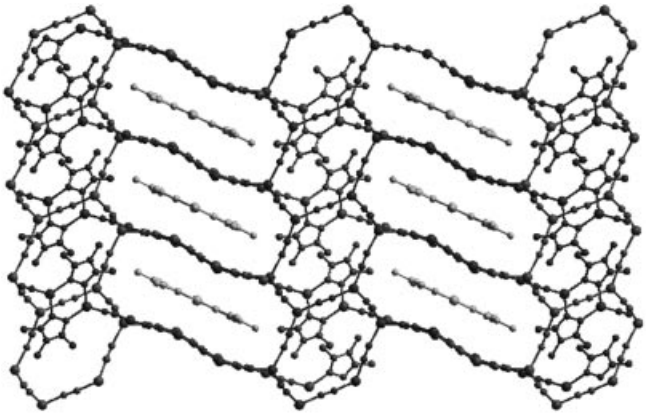

Figure 16. 3D + 1D structure of compound **7**, with the 1D polymer **B** filled in the two independent helical 3D polymers **A**.

Two independent helical substructures of polymer **A** $\{[Cu_6(CN)_6(dmtrz)]_n\}$ interweave into a 3D network with double-stranded helical channels that host 1D linear polymers **B** $\{[Cu_2(CN)_2(dmtrz)_2]_n\}$ to form a novel 3D supramolecular architecture (Figure 16).

This compound is interesting in that it contains two supramolecular isomers in the same crystal, infinite double helices with large channels in the spiral direction, and two kinds of helical channels with opposite chirality constructed by helical chains I and II in the same polymer.

Summary of the Structures

A series of compounds of a new copper cyanide/organoamine family have been synthesized by a hydrothermal method and structurally characterized. Compounds **1** and **2** contain a one-dimensional network. In contrast to the two one-dimensional chains mentioned above, compound **1** does not contain side-arms but has only N-heterocyclic ligands directly bound to the parent chains, whereas compound **2** has side arms, which represent an extra part with an additional {Cu(CN)} subunit. The cyanide groups only adopt μ_2-bridging modes in these compounds.

The 2D compound **3**, in which triazole ligands and cyanide groups all act as bridging ligands to link the copper atoms into a 2D structure, is obtained with the μ_3-bridging triazole ligand. This structure can be compared with that of **4**, which contains μ_2-dmtrz ligands instead of μ_3-triazole ligands, and therefore contains structurally different dimensionalities. The steric demands of the bulky substituents on the 3-, 4-, and 5-positions may be the cause of the change of coordination number around the copper atom. It has previously been pointed out that the use of triazole derivatives gives interesting coordination compounds.[5]

Compounds **5** and **6**, in which the cyanide groups exhibit two different coordination modes in a 3D structure, are obtained with the μ_4-bridging tetrazole ligand. In the structures of compounds **5** and **6**, which contain the polycyclic N-heterocyclic ligands 5-metta and 5-phtta, respectively, all the ligands are μ_4-bridging and link four copper atoms. Steric effects might be the major factors controlling the structures of these compounds, although the different coordination modes of the cyanide groups also affect the structural framework.

Although they contain the same ligand, two different structures are present in compounds **4** and **7**. One is a 3D network and the other is a 3D + 1D network. It can be seen that the different arrangement of the cyanide groups results in different dimensionalities. In compound **7**, all the cyanide groups adopt a μ_2-bridging coordination mode, while μ_2-bridging and μ_3-bridging modes are found in compound **4**. The versatility of the connectivity motifs linking the copper atoms therefore provides a rich structural chemistry.

Photoluminescent Properties

It is well known that numerous mono- and polynuclear Cu^I compounds show excellent luminescence properties.

Metal-to-ligand charge-transfer is the most common assignment of the lowest electronic excited state, although copper-centered emission, ligand-centered emission, and interligand charge-transfer are also possible.[25] We have studied the luminescence properties of compounds **1**–**7** (Figure 17). The emission spectra have a maximum at 523, 622, 508, 589, 505, and 481 nm, with an excitation maximum at 307, 348, 345, 316, 352, and 352 nm for **1**, **2**, **3**, **4**, **6**, and **7**, respectively. The emission may be tentatively assigned to a metal-to-ligand charge transfer (MLCT: Cu→CN) because the oxidation state of the copper atoms bridged by cyanide ions in these compounds is +1 and this is also consistent with the results of the IR spectra and is similar to the situation in other cyanide complexes.

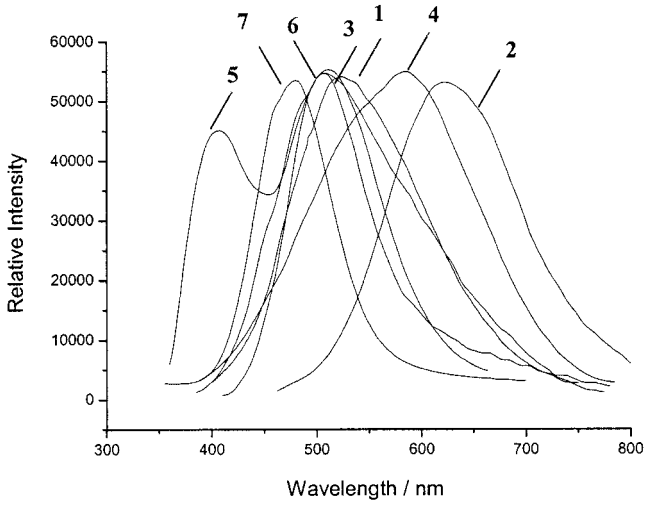

Figure 17. Emission spectra of compounds **1**–**7** measured in the solid state at room temperature.

The emission spectrum of compound **5** has a low-energy transition at around 408 nm and a high-energy one at around 502 nm, with an excitation maximum at 338 nm. The high-energy transition can be assigned as metal-to-ligand transfer (MLCT: Cu→CN), whereas the low-energy transition may be attributed to intraligand (π–π*) fluorescence in the 5-metta ligands, which is in reasonable agreement with literature examples.[26–28]

IR Spectra

The IR bands corresponding to the CN stretching vibrations for compounds **1**–**7** appear in the range 2080–2158 cm^{-1}, which is typical for bridging cyanide groups and higher than that of terminal cyanide ions (approx. 2050 cm^{-1}).[29] For compounds **1**, **5**, and **6** there is only one ν(CN) absorption, thus indicating the existence of one type of cyanide group in the crystal lattice, while there are two absorptions in compounds **2**–**4** and **7**, thus indicating the existence of two types of cyanide groups. Although the cyanide groups are only in μ_2-bridging modes in compounds **2** and **7**, the reason for the two absorptions might be the different distances of the Cu^I–C/N bond as the coordination number around copper(I) atoms increases. For cyanide-bridged Cu^I compounds, Cu^I–C/N distances are found to increase with coordination number around the copper(I) atoms. For instance, the Cu^I–C/N distances range from 1.82–1.86 Å for nearly linear two-coordinate systems whereas they increase to 1.92–1.98 Å in three-coordinate systems; ν(CN) increases as the Cu^I–CN distances decreases. This trend has also been observed for other compounds.[30,31]

Conclusions

We have obtained seven new copper cyanide/N-heterocycle compounds with a variety of one-, two-, three-, and one/three-dimensional frameworks by a hydrothermal method. We have found that organic ligands with specific geometric requirements affect the structure of these compounds. Triazole and tetrazole ligands bridge the copper centers to propagate a variety of structural styles that form multi-dimensional networks, while pyrazole and imidazole serve as terminal ligands that restrict the spatial extension of the structure. Other factors, such as the subtle interplay of metal coordination preferences, ligand type, spatial extension, and steric constraints, also play important roles in the formation of novel multidimensional open framework materials. The successful isolation of seven compounds demonstrates that it is possible to apply $K_3Fe(CN)_6$ as a precursor and other N-heterocyclic ligands to prepare coordination compounds with various structures under hydrothermal conditions. Some compounds display strong fluorescence emissions at different wavelengths, and these might be used as new emitting materials. The structure–function relationships of such components will begin to emerge and will provide further guidelines for synthetic methodologies.

Experimental Section

General Remarks: All syntheses were performed in poly(tetrafluoroethylene)-lined stainless steel autoclaves under autogenous pressure. Reagents were purchased commercially and were used without further purification. Elemental analyses for C and H were performed with an EA1110 CHNS-0 CE elemental analyzer. IR spectra (KBr pellets) were recorded with a Nicolet Magna 750FT-IR spectrometer. Fluorescence data were collected with an Edinburgh FL-FS920 TCSPC system.

General Method for the Preparation of Compounds 1–6: A mixture of CuCN (0.27 g, 3 mmol), $K_3Fe(CN)_6$ (0.32 g, 1 mmol), and the corresponding N-heterocyclic ligand (1 mmol; Scheme 1) in 15 mL of H_2O was stirred at room temperature for 20 min, then the mixture was transferred into a 25-mL Teflon-lined stainless steel vessel and the mixture was heated at 180 °C under autogenous pressure for 3 d. After the reaction mixture had slowly cooled to room temperature, suitable crystals for X-ray diffraction were produced, which were collected by filtration and washed with distilled water and dried in air.

$[Cu(CN)(dmpyz)]_n$ (1): Colorless prism-like crystals, (0.23 g; yield: 43%, based on Cu). $C_6H_8CuN_3$ (185.69): calcd. C 38.81, H 4.34, N 22.63; found C 38.92, H 4.36, N 22.71. IR (solid KBr pellet): $\tilde{\nu}$ = 339 (s), 2106 (s), 1570 (m), 1470 (m), 1284 (m), 1153 (m), 1037 (m), 978 (w), 779 (m), 679 (m), 654 (m), 579 (m), 445 (w), 427 (w) cm^{-1}.

$[Cu_2(CN)_2(imz)]_n$ (2): Colorless needle-like crystals (0.16 g; yield: 42%, based on Cu). $C_5H_4Cu_2N_4$ (247.19): calcd. C 24.29, H 1.63, N 22.66; found C 24.60, H 1.02, N 23.28. IR (solid KBr pellet): $\tilde{\nu}$ = 3346 (s), 3149 (m), 2146 (m), 2108 (s), 1635 (w), 1543 (m), 1508 (m), 1427 (m), 1257 (m), 1070 (s), 843 (w), 762 (m), 714 (m), 650 (m), 607 (m) cm^{-1}.

$[Cu_3(CN)(trz)_2]_n$ (3): Colorless prism-like crystals (0.11 g; yield: 30%, based on Cu). $C_5H_4Cu_3N_7$ (352.77): calcd. C 17.02, H 1.14, N 27.79; found C 17.32, H 1.48, N 27.42. IR (solid KBr pellet): $\tilde{\nu}$ = 3130 (m), 2102 (s), 2090 (s), 2069 (m), 1713 (m), 1506 (s), 1279 (s), 1205 (m), 1155 (s), 1066 (m), 1016 (m), 877 (m), 854 (m), 679 (m) cm^{-1}.

$[Cu_6(CN)_6(dmtrz)_3]_n$ (4): Colorless prism-like crystals (0.17 g; yield: 40%, based on Cu). $C_{18}H_{24}N_{18}Cu_6$ (873.79): calcd. C 24.74, H 2.77, N 28.85; found C 24.33, H 2.45, N 28.62. IR (solid KBr pellet): $\tilde{\nu}$ = 3552 (m), 3421 (m), 3049 (m), 2102 (vs), 2080 (vs), 1628 (m), 1421 (s), 1342 (m), 1205 (m), 1142 (m), 1051 (m), 847 (s), 777 (w), 723 (s), 633 (w), 559 (m) cm^{-1}.

$[Cu_2(CN)(5\text{-metta})]_n$ (5): Colorless prism-like crystals (0.10 g; yield: 30%, based on Cu). $C_3H_3N_5Cu_2$ (236.18): calcd. C 15.26, H 1.28, N 29.65; found C 15.67, H 1.46, N 29.82. IR (solid KBr pellet): $\tilde{\nu}$ = 2953 (w), 2484 (w), 2081 (s), 1497 (s), 1375 (m), 1254 (m), 1176 (m), 1147 (m), 1111 (w), 1049 (m), 710 (m) cm^{-1}.

$[Cu_2(CN)(5\text{-phtta})]_n$ (6): Colorless prism-like crystals (0.16 g; yield: 36%, based on Cu). $C_8H_5N_5Cu_2$ (298.25): calcd. C 32.22, H 1.69, N 23.48; found C 32.54, H 1.93, N 24.09. IR (solid KBr pellet): $\tilde{\nu}$ = 3421 (m), 3078 (m), 2133 (s), 1525 (m), 1454 (s), 1379 (m), 1159 (m), 1078 (m), 928 (w), 789 (m), 741 (s), 717 (s), 546 (w), 519 (w) cm^{-1}.

Preparation of $\{[Cu_6(CN)_6(dmtrz)]_2[Cu_2(CN)_2(dmtrz)_2]\}_n$ (7): This compound was synthesized by a procedure analogous to that described above but with CuCN (5.6 mmol), $K_3Fe(CN)_6$ (1 mmol), and dmtrz (1 mmol). Colorless platelike crystals (0.21 g; yield: 31%, based on Cu). $C_{30}H_{32}Cu_{14}N_{30}$ (1702.4): calcd. C 21.17, H 1.89, N 24.68; found C 21.39, H 2.14, N 24.96. IR (solid KBr pellet): $\tilde{\nu}$ = 3365 (m), 3323 (m), 3278 (m), 2158 (s), 2108 (s), 1616 (m), 1543 (m), 1419 (m), 1394 (m), 1263 (w), 1049 (w), 887 (m), 779 (m), 744 (m), 660 (w) cm^{-1}.

X-ray Crystallographic Study: Suitable single crystals of the compounds were carefully selected and glued to thin glass fibers with epoxy resin. Crystal structure measurements for compounds **1**–**7** were performed with a Rigaku Mercury CCD diffractometer with graphite-monochromated Mo-K_α radiation (λ = 0.71073 Å) at room temperature. The structures were solved by direct methods and refined on F^2 with the SHELXL-97 program.[32] For all compounds the μ_2-bridging cyanide group between two Cu^I atoms indicated disorder with respect to the C and N termini; this disorder was treated by adopting 50% C and N occupancies at those sites. The disordered C/N positions are labeled as X. All non-hydrogen atoms were refined with anisotropic displacement parameters, and the hydrogen atoms were treated as riding atoms using the SHELX-97 default parameters. For **2**, the imidazole hydrogen atoms were neither found nor calculated, and the disorder was treated by assuming half occupancies of the C and N atoms. The crystallographic data and details of refinements for compounds **1**–**7** are summarized in Table 1; selected bond lengths and angles are listed in Table 2. CCDC-284132 (**1**), -284133 (**2**), -284136 (**3**), -284137 (**4**), -284138 (**5**), -284139 (**6**), and -284140 (**7**) contain the supplementary crystallographic data for this paper. These data can be obtained free of charge from The Cambridge Crystallographic Data Centre via www.ccdc.cam.ac.uk/data_request/cif.

Table 1. Crystal and structural refinement data for compounds **1**–**7**.

Compound	**1**	**2**	**3**	**4**	**5**	**6**	**7**
Empirical formula	$C_6H_8CuN_3$	$C_5H_4Cu_2N_4$	$C_5H_4Cu_3N_7$	$C_{18}H_{24}Cu_6N_{18}$	$C_3H_3Cu_2N_5$	$C_8H_5Cu_2N_5$	$C_{30}H_{32}Cu_{14}N_{30}$
Formula mass	185.69	247.19	352.77	873.79	236.18	298.25	1702.42
Crystal system	orthorhombic	orthorhombic	monoclinic	triclinic	orthorhombic	monoclinic	monoclinic
Space group	*Pnma*	*Pnma*	*C*2/*m*	$P\bar{1}$	*Pbam*	*C*2/*c*	*C*2/*c*
a [Å]	8.777(2)	6.9901(6)	14.0944(3)	11.1042(2)	7.2307(5)	11.123(9)	42.347(15)
b [Å]	6.6410(19)	8.5874(7)	11.2119(3)	11.2046(3)	13.4943(11)	12.780(9)	8.569(3)
c [Å]	12.716(3)	13.0732(11)	13.0843(4)	13.7862(2)	5.9352(5)	8.133(6)	14.490(5)
α [°]	90	90	90	69.565(9)	90	90	90
β [°]	90	90	113.684(2)	74.161(10)	90	125.231(8)	108.758(6)
γ [°]	90	90	90	65.069(9)	90	90	90
V [Å^3]	741.2(3)	784.74(11)	1893.50(9)	1441.48(5)	579.12(8)	944.3(13)	4979(3)
Z	4	4	8	2	4	4	4
$D_{calcd.}$ [g·cm^{-3}]	1.664	2.075	2.475	2.013	2.709	2.098	2.271
F(000)	376	472	1360	864	456	584	3312
Absorption coefficient [mm^{-1}]	2.867	5.351	6.649	4.392	7.249	4.470	5.903
θ range for data collection [°]	2.82–25.03	3.12–27.48	1.70–25.02	3.18–27.48	4.13–27.48	3.01–27.47	3.01–27.49
Reflections collected	1711	5686	2923	11297	4169	3511	18598
Unique reflections	695	953	1752	6529	724	1080	5684
R(int)	0.0368	0.0225	0.0260	0.0235	0.0303	0.0244	0.0443]
Parameters	61	60	151	379	54	70	337
Goodness-of-fit on F^2	1.006	1.018	1.079	1.052	1.055	1.054	1.095
R_1[a]	0.0697	0.0389	0.0514	0.0394	0.0203	0.0220	0.0448
wR_2 [$I > 2\sigma(I)$][b]	0.1560	0.1064	0.1163	0.0937	0.0543	0.0651	0.1221
R_1[a]	0.0800	0.0420	0.0558	0.0550	0.0211	0.0243	0.0519
wR_2 (all data)	0.1618	0.1085	0.1192	0.1024	0.0549	0.0663	0.1269

[a] $R_1 = \Sigma(|F_o| - |F_c|)/\Sigma|F_o|$. [b] $wR_2 = [\Sigma w(F_o^2 - F_c^2)^2/\Sigma w(F_o^2)^2]^{0.5}$.

Table 2. Selected bond lengths [Å] and angles [°] for compounds **1**–**7**. Symmetry transformations used to generate equivalent atoms are given as footnotes.

Compound **1**[a]					
Cu(1)–X(6)	1.870(11)	Cu(1)–X(7)^{I}	1.986(8)	X(6)–Cu(1)–X(7)^{I}	125.0(4)
Cu(1)–N(1)	1.988(7)	X(6)–Cu(1)–N(1)	136.6(4)	N(1)–Cu(1)–X(7)^{I}	98.4(3)
Compound **2**[b]					
N(1)–Cu(1)	1.920(4)	N(4)–Cu(2)	1.877(5)	X(2)–Cu(1)–X(1)	119.94(14)
X(2)–Cu(1)	1.916(5)	X(3)–Cu(2)–N(4)	170.1(3)	X(1)^{I}–Cu(1)–X(1)	120.1(3)
X(3)–Cu(2)	1.843(6)				
Compound **3**[c]					
Cu(1)–C(3)^{I}	1.955(10)	Cu(5)–N(7)	2.000(6)	N(9)^{III}–Cu(2)–N(9)	112.0(3)
Cu(1)–N(10)	2.016(6)	Cu(5)–N(2)^{VI}	1.888(9)	N(4)–Cu(3)–N(6)	123.34(19)
Cu(1)–C(3)^{II}	2.221(11)	Cu(6)–N(8)	1.867(6)	N(6)–Cu(3)–N(6)^{IV}	112.3(4)
Cu(2)–X(1)	1.882(10)	C(3)^{I}–Cu(1)–N(10)	114.3(2)	N(5)^{II}–Cu(4)–N(5)^{V}	178.0(4)
Cu(2)–N(9)	1.973(6)	N(10)–Cu(1)–N(10)^{III}	108.3(3)	X(2)^{VI}–Cu(5)–N(7)	124.27(18)
Cu(3)–N(4)	1.887(10)	C(3)^{I}–Cu(1)–C(3)^{II}	107.5(3)	N(7)^{VI}–Cu(5)–N(7)	110.2(3)
Cu(3)–N(6)	1.977(6)	N(10)–Cu(1)–C(3)^{II}	105.9(2)	N(8)–Cu(6)–N(8)^{VI}	176.7(4)
Cu(4)–N(5)^{II}	1.864(6)	X(1)–Cu(2)–N(9)	123.41(17)		
Compound **4**[d]					
Cu(1)–N(14)	1.895(3)	Cu(5)–X(22)	1.993(3)	X(23)^{I}–Cu(4)–X(18)	104.79(14)
Cu(1)–X(24)	1.898(4)	Cu(5)–C(13)^{III}	2.015(4)	X(23)^{I}–Cu(4)–C(20)	112.50(16)
Cu(1)–X(16)	1.991(4)	Cu(5)–C(13)^{IV}	2.258(4)	X(18)–Cu(4)–C(20)	110.66(14)
Cu(2)–X(15)	1.896(4)	Cu(6)–X(21)	1.908(4)	X(18)–Cu(4)–C(20)II	111.78(15)
Cu(2)–N(5)	1.966(3)	Cu(6)–N(9)	1.986(3)	C(20)–Cu(4)–C(20)^{II}	108.86(13)
Cu(2)–N(2)	2.007(3)	N(14)–Cu(1)–X(24)	135.01(15)	N(19)–Cu(5)–X(22)	107.06(14)
Cu(3)–X(17)	1.889(4)	N(14)–Cu(1)–X(16)	114.28(14)	N(19)–Cu(5)–C(13)^{III}	112.37(15)
Cu(3)–N(1)	1.972(3)	X(24)–Cu(1)–X(16)	110.55(15)	X(22)–Cu(5)–C(13)^{III}	117.16(14)
Cu(3)–N(6)	2.014(3)	X(15)–Cu(2)–N(5)	128.34(16)	N(19)–Cu(5)–C(13)^{IV}	105.42(14)
Cu(4)–X(23)^{I}	1.967(3)	X(15)–Cu(2)–N(2)	121.42(14)	X(22)–Cu(5)–C(13)^{IV}	106.64(14)
Cu(4)–X(18)	2.007(3)	N(5)–Cu(2)–N(2)	110.19(12)	C(13)^{III}–Cu(5)–C(13)^{IV}	107.44(11)
Cu(4)–C(20)	2.055(4)	X(17)–Cu(3)–N(1)	130.91(14)	X(21)–Cu(6)–N(9)	132.72(15)
Cu(4)–C(20)^{II}	2.142(4)	X(17)–Cu(3)–N(6)	118.08(14)	X(21)–Cu(6)–N(10)^{V}	117.13(15)
Cu(5)–N(19)	1.979(3)	N(1)–Cu(3)–N(6)	110.87(12)	N(9)–Cu(6)–N(10)^{V}	110.11(12)
Compound **5**[e]					
Cu(1)–N(3)	1.978(1)	N(3)–Cu(1)–N(3)^{II}	141.89(8)	N(4)–Cu(2)–C(1)IV	102.41(8)
Cu(1)–N(2)	1.993(2)	N(3)–Cu(1)–N(2)	109.03(4)	N(4)–Cu(2)–C(1)^{V}	114.74(9)
C(1)–Cu(2)^{I}	2.096(2)	N(2)–C(1)–Cu(2)^{I}	145.61(5)	C(1)^{IV}–Cu(2)–C(1)^{V}	111.86(8)
N(4)–Cu(2)	2.011(1)	N(4)^{III}–Cu(2)–N(4)	111.16(8)	N(4)–Cu(2)–Cu(2)^{VI}	124.42(4)
Cu(2)–C(1)^{IV}	2.096(2)				
Compound **6**[f]					
X(1)–Cu(1)	1.877(2)	C(6)–N(3)–Cu(1)	131.67(14)	X(1)–Cu(1)–N(2)	114.73(9)
N(2)–Cu(1)	2.088(1)	N(2)^{I}–N(3)–Cu(1)	120.13(12)	N(3)–Cu(1)–N(2)	102.91(7)
N(3)–Cu(1)	1.967(2)	X(1)–Cu(1)–N(3)	140.46(9)		
Compound **7**[g]					
X(5)–Cu(2)	1.885(5)	X(11)–Cu(3)	1.886(4)	N(2)–Cu(2)–N(2)^{II}	110.99(19)
X(12)–Cu(4)	1.846(3)	X(13)–Cu(4)	1.857(5)	X(11)–Cu(3)–N(8)	123.60(15)
X(14)–Cu(5)	1.839(4)	X(15)–Cu(5)	1.855(4)	X(11)–Cu(3)–N(10)	127.48(15)
X(16)–Cu(6)	1.844(4)	X(17)–Cu(6)	1.866(4)	N(8)–Cu(3)–N(10)	108.59(12)
X(18)–Cu(7)	1.927(4)	X(19)–Cu(7)	1.993(4)	X(12)–Cu(4)–X(13)	168.8(2)
X(20)–Cu(8)	1.895(4)	X(23)–Cu(8)	1.905(4)	X(14)–Cu(5)–X(15)	170.4(2)
X(21)–Cu(7)	1.916(4)	Cu(8)–X(22)^{I}	1.971(4)	X(16)–Cu(6)–X(17)	166.3(2)
N(1)–Cu(1)	1.992(3)	X(6)–Cu(1)–N(1)	124.82(9)	X(21)–Cu(7)–X(18)	133.42(18)
N(2)–Cu(2)	1.970(3)	X(6)–Cu(1)–N(1)^{II}	124.82(9)	X(21)–Cu(7)–X(19)	111.59(17)
N(6)–Cu(1)	1.897(6)	N(1)–Cu(1)–N(1)^{II}	110.35(19)	X(18)–Cu(7)–X(19)	111.21(18)
N(8)–Cu(3)	1.993(3)	X(5)–Cu(2)–N(2)	124.51(9)	X(20)–Cu(8)–X(23)	124.9(2)
N(10)–Cu(3)	2.001(3)	X(5)–Cu(2)–N(2)^{II}	124.51(9)	X(20)–Cu(8)–X(22)^{I}	118.52(16)
				X(23)–Cu(8)–X(22)^{I}	115.85(19)

[a] I: *x* – 1/2, *y*, –*z* + 3/2. [b] I: –*x* + 2, –*y*, –*z*. [c] I: *x* – 1/2, *y* – 1/2, *z* – 1; II: –*x* + 1/2, –*y* + 1/2, –*z* + 2; III: *x*, –*y*, *z*; IV: *x*, –y + 1, *z*; V: –*x* + 1/2, *y* + 1/2, –*z* + 2; VI: *x* – 1/2, *y* + 1/2, *z*. [d] I: *x*, *y*, *z* + 1; II: –*x* + 2, –*y* + 1, –*z* + 1; III: *x* + 1, *y* – 1, *z* + 1; IV: –*x* + 1, –*y* + 1, –*z*; V: –*x* + 1, –*y*, –*z* + 2. [e] I: –*x* + 1/2, *y* – 1/2, –*z*; II: *x*, *y*, –*z*; III: –*x* + 1, –*y* + 1, *z*; IV: *x* + 1/2, –*y* + 1/2, *z*; V: –*x* + 1/2, *y* + 1/2, –*z*; VI: –*x* + 1, –*y* + 1, –*z*. [f] I: –*x* + 1/2, –*y* + 1/2, –*z* + 2. [g] I: *x*, –*y* – 3, *z* + 1/2; II: –*x*, *y*, –*z* – 1/2.

Supporting Information (see footnote on the first page of this article): Packing diagram of **3**–**6** and additional figure of **7**.

Acknowledgments

This work was supported by the 973 program of the MOST (001CB108906), the National Science Foundation of China (20425313, 90206040, 20333070, and 20303021), the NSF of Fujian, and the Chinese Academy of Sciences.

[1] L. Toma, R. Lescouezec, J. Vaissermann, F. S. Delgado, C. Ruiz-Perez, R. Carrasco, J. Cano, F. Lloret, M. Julve, *Chem. Eur. J.* **2004**, *10*, 6130–6145.
[2] M. Verdaguer, A. Bleuzen, V. Marvaud, J. Vaissermann, M. Seuleiman, C. Desplanches, A. Scuiller, C. Train, R. Garde, G. Gelly, C. Lomenech, I. Rosenman, P. Veillet, C. Cartier, F. Villain, *Coord. Chem. Rev.* **1999**, *190*, 1023–1047.
[3] M. Ohba, H. Okawa, *Coord. Chem. Rev.* **2000**, *198*, 313–328.
[4] T. Korzeniak, K. Stadnicka, R. Pelka, M. Balanda, K. Tomala, K. Kowalski, B. Sieklucka, *Chem. Commun.* **2005**, 2939–2941.
[5] L. Yi, B. Ding, B. Zhao, P. Cheng, D. Z. Liao, S. P. Yan, Z. H. Jiang, *Inorg. Chem.* **2004**, *43*, 33–43.
[6] J. M. Zheng, S. R. Batten, M. Du, *Inorg. Chem.* **2005**, *44*, 3371–3373.
[7] P. V. Bernhardt, F. Bozoglian, B. P. Macpherson, *Coord. Chem. Rev.* **2005**, *249*, 1902–1916.
[8] D. F. Shriver, *Struct. Bonding (Berlin)* **1966**, *1*, 32–58.
[9] H. Zhang, J. Cai, X. L. Feng, B. H. Ye, X. Y. Li, L. N. Ji, *J. Chem. Soc., Dalton Trans.* **2000**, 1687–1688.
[10] D. J. Chesnut, A. Kusnetzow, R. Birge, J. Zubieta, *Inorg. Chem.* **1999**, *38*, 5484–5494.
[11] E. Colacio, J. M. Dominguez-Vera, F. Lloret, J. M. M. Sanchez, R. Kivekas, A. Rodriguez, R. Sillanpaa, *Inorg. Chem.* **2003**, *42*, 4209–4214.
[12] a) E. Colacio, R. Kivekas, F. Lloret, M. Sunberg, J. S. Varela, M. Bardaji, A. Laguna, *Inorg. Chem.* **2002**, *41*, 5141–5149; b) E. Colacio, A. Debdoubi, R. Kivekas, A. Rodriguez, *Eur. J. Inorg. Chem.* **2005**, 2860–2868.
[13] D. T. Cromer, A. C. Larson, *Acta Crystallogr., Sect. B* **1972**, *28*, 858–861.
[14] Crystallographic data for $K[Cu(CN)_3]_n \cdot H_2O$: mononclinic, space group $P2_1/c$, a = 12.034(2), b = 8.2249(15), c = 7.4987(14) Å, β = 96.637(4)°, V = 737.3(2) Å^3, Z = 4, ρ = 2.363 g cm^{-3}, $F(000)$= 504, μ(Mo-K_α) = 6.259 mm^{-1}, GOF = 1.129. Of 2442 total reflections collected, 1285 were unique [R(int)= 0.0477] R_1 (wR_2) = 0.0867 (0.1734) for 91 parameters. CCDC-284904 contains the supplementary crystallographic data for this paper. These data can be obtained free of charge from The Cambridge Crystallographic Data Centre via www.ccdc.cam.ac.uk/data_request/cif.
[15] P. M. Forster, A. R. Burbank, C. Livage, G. Férey, A. K. Cheetham, *Chem. Commun.* **2004**, 368–369.
[16] A. J. Blake, N. R. Brooks, N. R. Champness, P. A. Cooke, A. M. Deveson, D. Fenske, P. Hubberstey, W.-S. Li, M. Schröder, *J. Chem. Soc., Dalton Trans.* **1999**, 2103–2110.
[17] J. R. Black, N. R. Champness, W. Levason, G. Reid, *J. Chem. Soc., Chem. Commun.* **1995**, 1277–1278.
[18] a) A. Rujiwatra, C. J. Kepert, M. J. Rosseinsky, *Chem. Commun.* **1999**, 375–376; b) M. Kondo, T. Yoshitomi, K. Seki, H. Matsuzaka, S. Kitagawa, *Angew. Chem. Int. Ed. Engl.* **1997**, *36*, 1725–1727.
[19] M. J. Zaworotko, *Chem. Commun.* **2001**, 1–2.
[20] Z.-Y. Fu, X.-T. Wu, J.-C. Dai, L.-M. Wu, C.-P. Cui, S.-M. Hu, *Chem. Commun.* **2001**, 1856–1857.
[21] a) J.-C. Dai, X.-T. Wu, Z.-Y. Fu, S.-M. Hu, W.-X. Du, C.-P. Cui, L.-M. Wu, H.-H. Zhang, R.-Q. Sun, *Chem. Commun.* **2002**, 12–13; b) R. E. Melendez, C. V. K. Sharma, M. J. Zaworotko, C. Bauer, R. D. Rogers, *Angew. Chem. Int. Ed. Engl.* **1996**, *35*, 2213–2215.
[22] R. I. Papasergio, C. L. Raston, A. H. White, *J. Chem. Soc., Dalton Trans.* **1987**, 3085–3091.
[23] C. M. Che, Z. Mao, V. M. Miskowski, M. C. Tse, C. K. Chan, K. K. Cheung, D. L. Phillips, K. H. Leung, *Angew. Chem. Int. Ed.* **2000**, *39*, 4084–4086.
[24] J. Beck, J. Strahle, *Angew. Chem. Int. Ed. Engl.* **1985**, *24*, 409–410.
[25] M. Vitale, P. C. Ford, *Coord. Chem. Rev.* **2001**, *219*, 3–16.
[26] M. Henary, J. L. Wootton, S. I. Khan, J. I. Zink, *Inorg. Chem.* **1997**, *36*, 796–801.
[27] B. W. Pfennig, A. B. Bocarsly, *J. Phys. Chem.* **1992**, *96*, 226–233.
[28] C. Dlaz, A. Arancibia, *Inorg. Chim. Acta* **1998**, *269*, 246–263.
[29] K. Nakamoto, *Infrared and Roman Spectra of Inorganic Coordination Compounds*, 4th ed., Wiley, New York, **1986**, p. 272.
[30] G. A. Bowmaker, J. C. Effendy, C. E. Reid, F. Rickard, B. W. Skelton, A. H. White, *J. Chem. Soc., Dalton Trans.* **1998**, 2139–2146.
[31] D. J. Chesnut, A. Kusnetzow, R. Birge, J. Zubieta, *J. Chem. Soc., Dalton Trans.* **2001**, 2581–2586.
[32] G. M. Sheldrick, *SHELXS97, Program for Solution of Crystal Structures*, University of Göttingen, Germany, **1997**.

Received: November 3, 2005
Published Online: April 20, 2006

